CHAPTER IV

RESULTS AND DISCUSSION

4.1 Morphology of electrospun SF nanofibers

4.1.1 Effect of silk polymer concentration on fiber diameters

In order to study the effect of polymer solution concentration on fiber morphology, SF concentrations of 42, 44, 46, 48, 50 and 52 % (w/v) were used. While the SF concentrations were varied, the other parameters were kept constant (needle gauge = 20, electrospinning distance = 15 cm, and electrospinning voltage = 25 kV).

The results of this study are shown in Table 4.1. As indicated, no fibers were formed when the SF concentration was less than 44 % (w/v) for a specific electric field and spinning distance. However, when the SF concentration was increased to 44% (w/v), the smallest fiber diameter, being around 250 nm, are formed with significant beads connected with the fibers in this concentration. The concentrations of 44-52 % (w/v) proceeded in a consistent manner to produce nanofibers with a progressively decreased occurrence of beads with an increased concentration. The continuous nanofibers can be obtained at the concentration above 50 % (w/v). However at 50 % w/v concentration, nanofibers without beads were generated and the electrospun fibers from this concentration had an average diameter of 329 nm.

These results can be explained that, at low concentration or low viscosity, stable jet cannot be formed, which is well-known to play a major role in the formation of beads. If polymer concentration is too low, fibers are not formed but only droplets are produced due to the jet breaks up into droplets known as the electrospray [33]. Based on these results an optimal polymer solution concentration of 50 % (w/v) was used to further study the influence of applied voltage.

Table 4.1 SEM micrographs and fiber diameter of as-spun SF by electrospinning at various SF concentrations with a constant electrospinning distance of 15 cm at applied voltage of 25 kV.

Concentration% (w/v)	**SEM micrographs**	**Average diameter (nm)**
42	No fiber formation	-
44	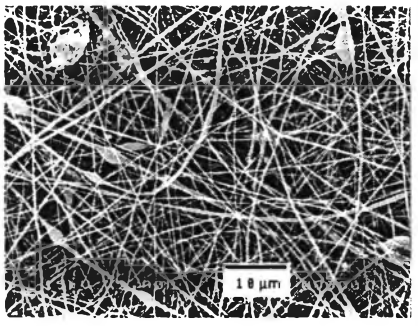 (2000 X)	250 ± 74
46	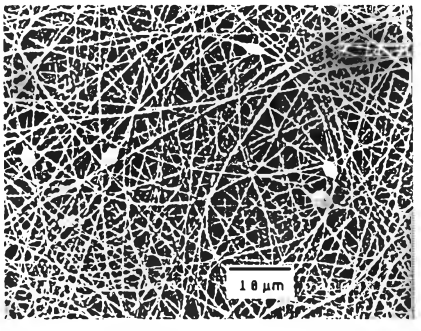 (2000 X)	264 ± 82
48	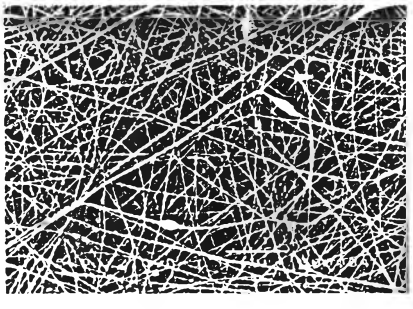 (2000 X)	272 ± 92

Table 4.1 (Continued)

Concentration% (w/v)	SEM micrographs	Average diameter (nm)
50	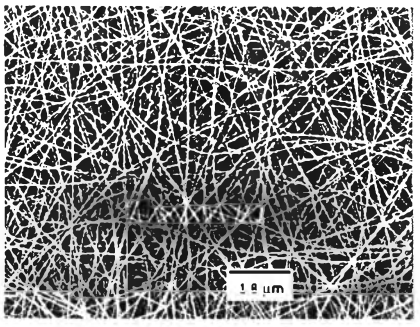 (2000 X) 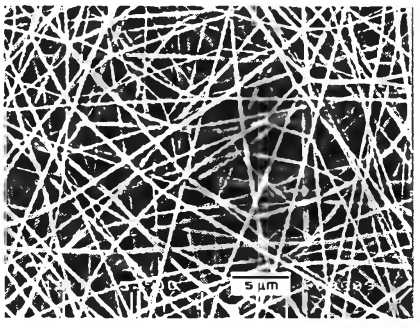 (3500 X)	329 ± 85
52	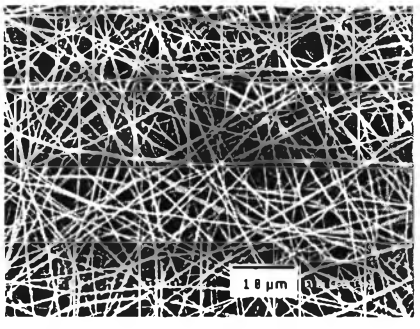 (2000 X) 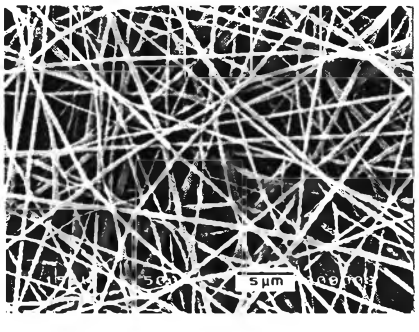 (3500 X)	417 ± 72

4.1.2 Effect of applied voltage on fiber diameters

The effect of applied voltage was also investigated in this research. To study this effect, applied voltages were varied from 15 to 30 kV at the SF concentration of 50 % (w/v) and collection distance of 15 cm.

Table 4.2 showed the morphologies of the as-spun SF obtained at varying voltages. It can be seen that at low applied voltages of 15 and 20 kV (Table 4.2(a), (b)), electrospinning of the solution generated beads and fibers with beads, respectively, because the voltages are still lower than the surface tension of SF solution. At 25 kV (Table 4.2 (c)), the voltage was applied to the critical voltage value then the jets were initiated, the continuous nanofibers without bead defects could be obtained. Because the electric field was high enough to overcome the surface tension of SF solution. At the high voltage of 30 kV (Table 4.2 (d)), the bead defects could be obtained in the fiber mats because the flow of the solution to a syringe needle tip did not match the rate at which the solution was being removed [34]. Based on these results, the suitable conditions to produce electrospun SF fibers as a scaffolding material for keratinocyte and fibroblast cells in this research were 50% (w/v) SF solution at the applied voltage of 25 kV with an electrospinning distance of 15 cm.

Table 4.2 SEM micrographs (2000X) and fiber diameter of as-spun SF fabricated fabricated by electrospinning at various applied voltages, the concentration of 50 % (w/v) with a constant spinning distance of 15 cm.

Applied voltages (kV)	SEM micrographs	Average diameter (nm)
15	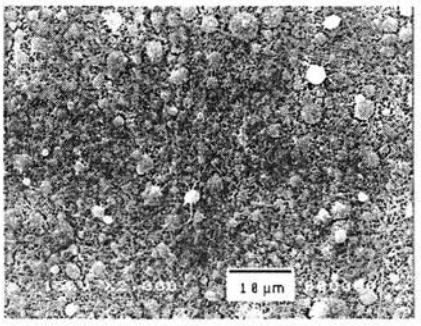 (a)	-
20	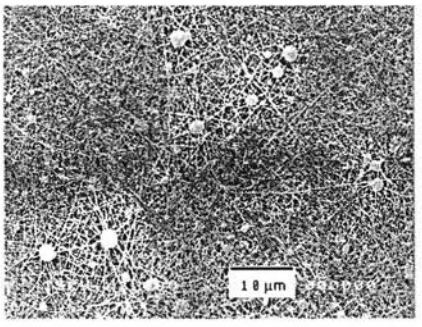 (b)	234 ± 54
25	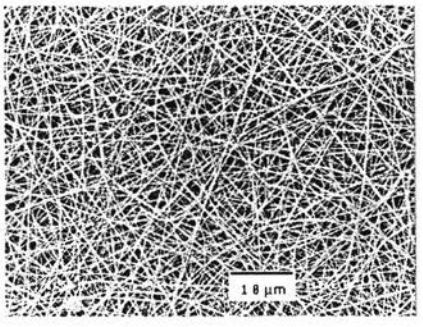 (c)	333 ± 44

Table 4.2(Continued)

Applied voltages (kV)	**SEM micrographs**	**Average diameter (nm)**
30	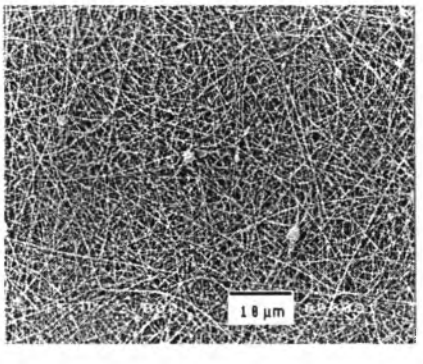 **(d)**	244 ± 65

4.2 Surface characteristic of neat and HA coated as-spun SF fiber mats

In order to confirm the coating of hyaluronic acid on as-spun SF, FT-IR and ATR-IR spectroscopy were performed and IR spectra of the neat as-spun SF fibers, HA-coated as-spun SF fibers, and pure HA powder were shown in Figure 4.1(A), (B), and (C), respectively.

The neat as-spun SF fiber mats showed absorption bands at 1623 cm^{-1} (amide I), 1528 cm^{-1} (amide II), 1250 cm^{-1} (amide III) and 680 cm^{-1} (amide V), all being assigned to β-sheet conformation [27,35-38]. The peaks of pure HA powder at 3420, 2901, 1618, 1409, 1368, 1156, 1042, and 617 corresponded to the stretching vibration of –OH–, -CH-, C=O (carboxyl amide I group), CH_3 (both 1409 and 1368), –C–O–C– bond, –O–CH– bond, and CH_2 bond.

The IR spectrum of HA-coated electrospun SF fibers showed significant difference with as-spun SF in absorption bands at 3288, 1738, 1626, 1519, 1444, 1366, and 1229 cm^{-1} can be assigned to –OH–, C=O, amide I , amide II, CH_3 (both 1444 and 1366), and amide III and can also be found in both neat as-spun SF fibers and of HA-coated as-spun SF fibers.

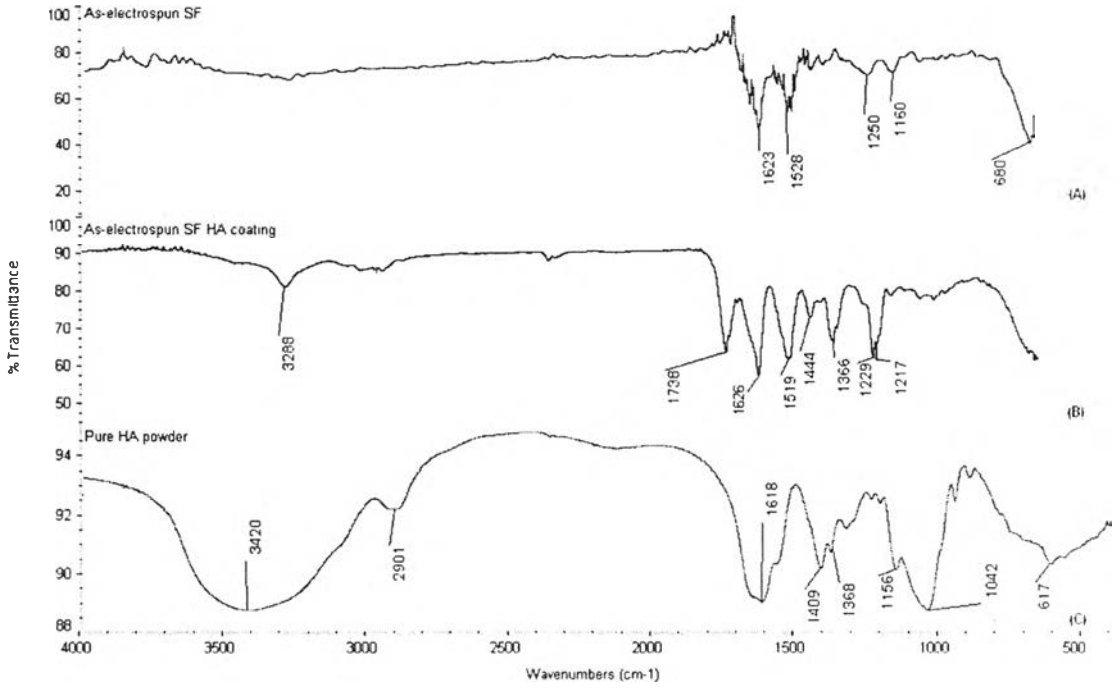

Figure 4.1 ATR-IR and FT-IR spectra of (A) neat as-spun SF fibers, (B) HA-coated as-spun SF fibers, and (C) pure HA powder

4.3 Thermogravimetric analysis (TGA)

Figure 4.2 showed the thermogravimetric curves of neat as-spun SF fibers, pure hyaluronic acid powder (HA), and HA-coated as-spun SF fibers (SF-HA). Each sample was tested under nitrogen atmosphere at a heating rate of 10 °C/min.

The TGA curve of as-spun SF fibers and pure HA powder showed a characteristic transition band at the temperature between 80 °C and 100 °C; this may be due to the evaporation of water content in the as-spun SF fibers and pure HA powder induced by heating. Although as-spun SF fibers were sufficiently dry before measurement, the bound water does not evaporate because of the water molecules which are bound to SF molecules through hydrogen bonds (weight loss of 8-10%). HA has high capacity water-sorption and water retention.

As the temperature increased further, the as-spun SF fibers remained stable until approximately 270 °C, when the TGA curve started to decrease indicating the beginning of the thermal decomposition. Afterwards, a greater weight loss was occurred to approximately 320 °C. This decomposition behavior is associated with the breakdown of side groups of amino acid residues as well as the cleavage of peptide bonds of the as-spun SF fiber [39].

For pure HA powder, the thermal decomposition of a greater weight loss ranged from 230 to 280 °C. Interestingly SF-HA, showed greater weight loss from 120 to 260 °C due to decomposition of HA that was coated on electrospun SF fiber and its thermogram did not show the evaporation of water content around 100 °C due to its degree of cross-linking between the chain of SF and HA. The second weight loss seemed to take place at the temperature about 320 °C, similar with that of as-spun SF fibers. The SF-HA showed faster degradation curve, indicating lower stability than as-spun SF fibers.

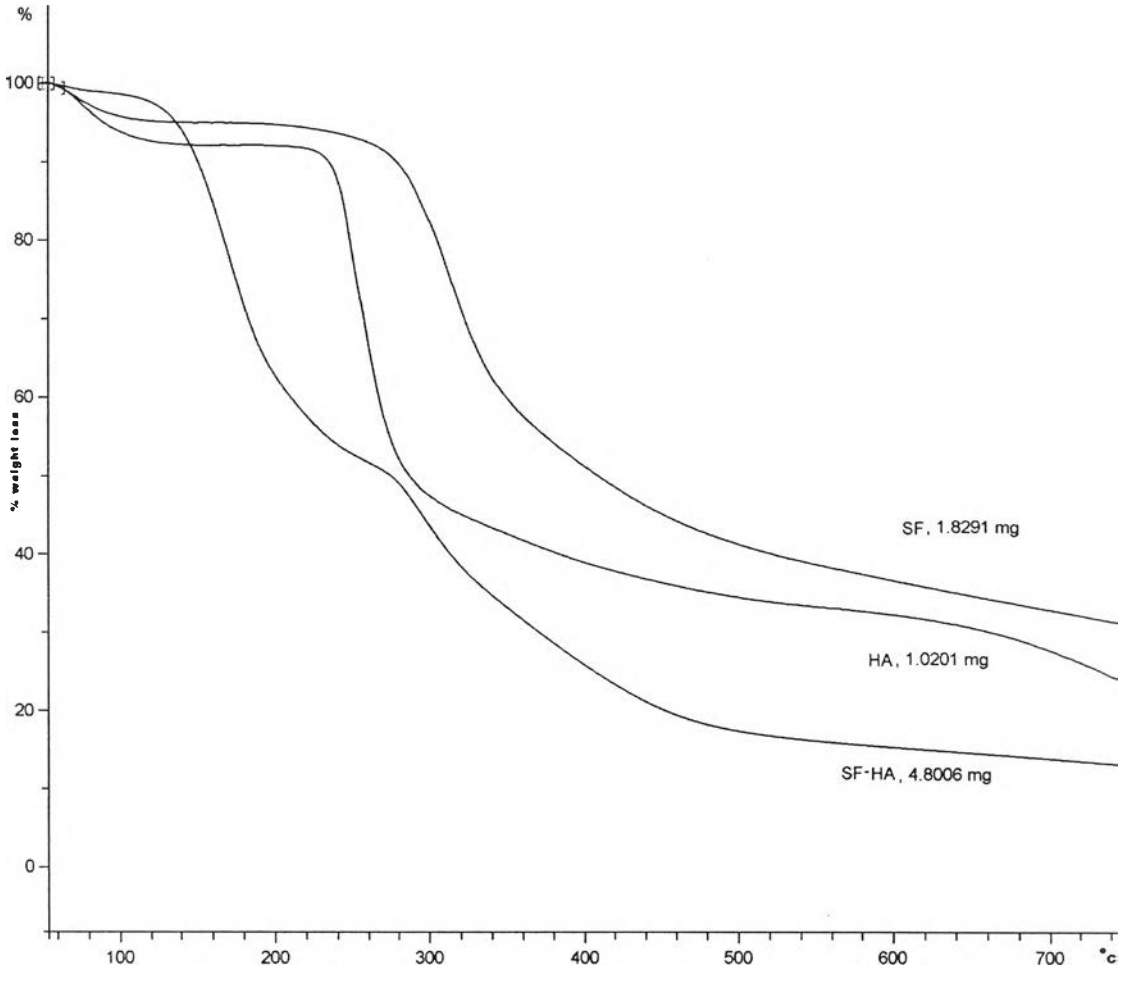

Figure 4.2 Thermogravimetric diagram of as-spun SF fibers, pure HA powder (HA), and HA-coated as-spun SF fibers (SF-HA)

4.4 Cytotoxicity

To determine biocompatibility of the as-prepared materials as scaffolds for tissue engineering, the MTT assay was performed to monitor the cytotoxicity of the as-prepared materials. The quantities of the number of viable cells were listed in Table 4.3 and the normalized results are shown in Figure 4.3, which shows the cytotoxicity of each materials compared with the tissue-culture polystyrene plate (TCPS; control). As indicated in this figure, there is no significant difference of absorbance values in comparison with the control. All results clearly showed that as-prepared materials were nontoxic to L929 cells, suggesting that these materials can be a good candidate to be used as scaffolds.

Table 4.3 Data shows the quantities (%) of percentage of viable L929 cells on each scaffolding material comparison with control.

Type	Absorbance	Percentage of viable cell (% with control)
Control	0.872	100 ± 1
SF film	0.823	94 ± 3
SF fiber	0.837	96 ± 0.8
SF-HA	0.887	102 ± 3

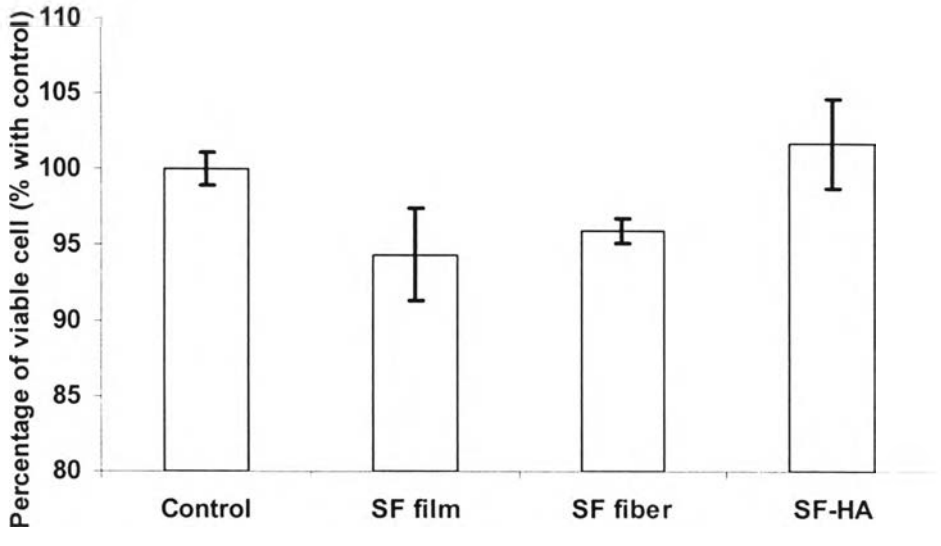

Figure 4.3 Cytotoxicity of as-prepared materials to L929 cells in comparison with control.

4.5 Cell attachment and proliferation

Further investigation was carried out to evaluate the biocompatibility of the as-spun SF nanofibers and HA-coated SF nanofibers in terms of the attachment and the proliferation of cells that were seeded on these scaffolds. The cells used were human foreskin fibroblasts (HFF) and immortalized human keratinocytes (HaCaT). These cells are selected for testing with scaffold in skin tissue engineering [9,24,26-27,39].

4.5.1 HaCaT cells

The attachment and proliferation of HaCaT on materials can be observed from SEM micrographs in Table 4.4 and 4.6, respectively.

According to Table 4.4, these images can be described that up to 6 hours in culture, most of HaCaT cells seeded on films and control were still in round shape. However, cells on SF fibers and SF-HA fibers started to show the lamellipodia at 6 h expanded more than films and controls at 6 hours in culture. When compared between SF-HA fibers and SF fibers, the results indicated that cell shape on SF-HA fibers were flatter than SF at all time in culture.

Table 4.4 SEM micrographs (3500X) of HaCaT cells attached on the surface of SF film, as-spun SF and HA-coated SF fibrous (SF-HA) scaffolds comparison with control. The scale bar shown is 5 μm.

	Control	SF Film	SF fiber	SF-HA
2 h	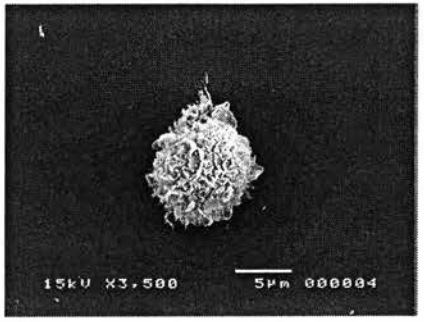	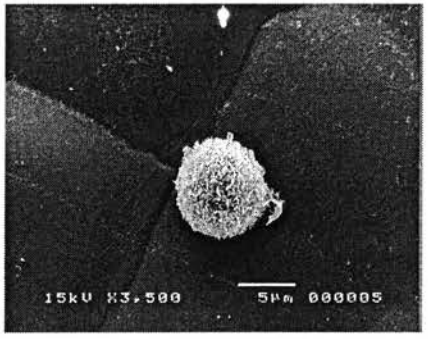	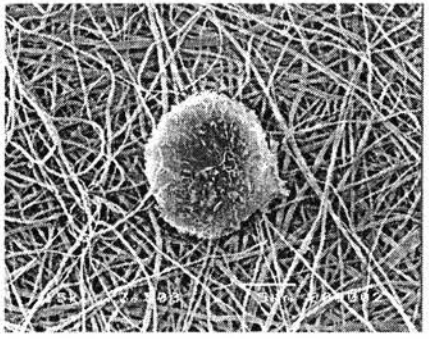	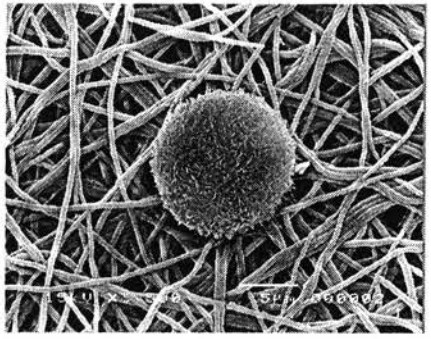
4 h	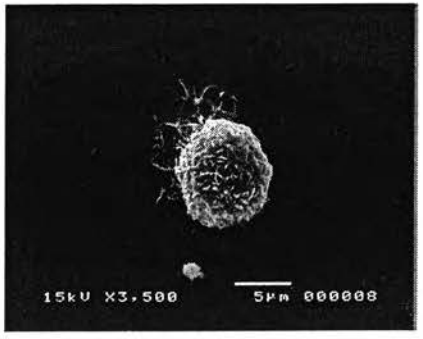	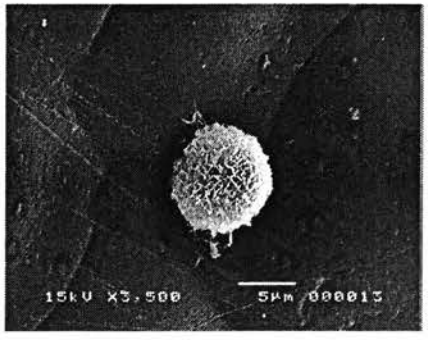	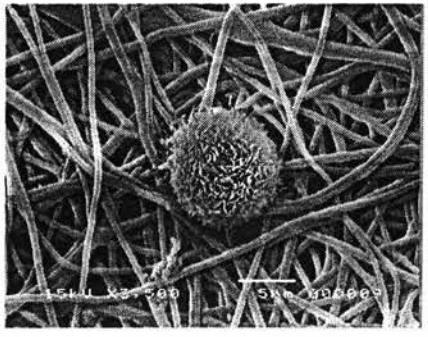	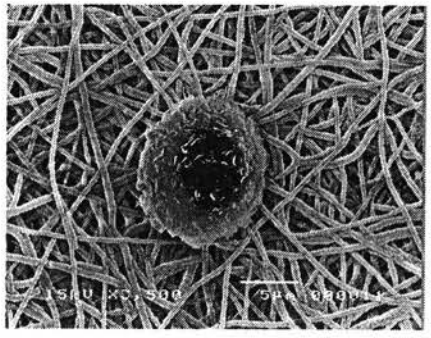

Table 4.4 (continued)

	Control	SF Film	SF fiber	SF-HA
6 h	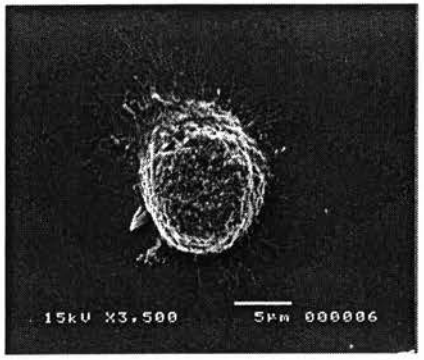	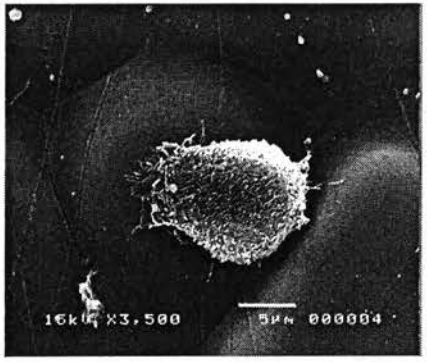	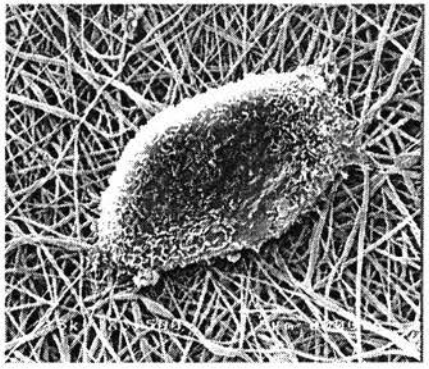	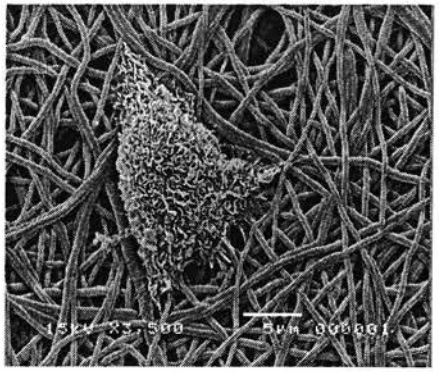

The results of SEM micrographs corresponded to the studying a number of viable cells by measuring the UV absorbance from MTT assay. This assay indicates viable cells, and cellular dehydrogenase activity, which converts the MTT substrate to a colored formazan product, indirectly related to cell number.

Table 4.5 Data shows the quantities (%) of percentage of viable HaCaT cell attached on each scaffolding material comparison with control.

Type	Absorbance			Percentage of viable cell (% with control)		
	2 h	4 h	6 h	2 h	4 h	6 h
Control	0.044	0.082	0.130	100 ± 2	186 ± 4	295 ± 2
SF film	0.114	0.121	0.117	259 ± 16	275 ± 34	266 ± 2
SF fiber	0.122	0.137	0.127	277 ± 34	311 ± 9	289 ± 16
SF-HA	0.223	0.262	0.166	507 ± 64	595 ± 27	377 ± 14

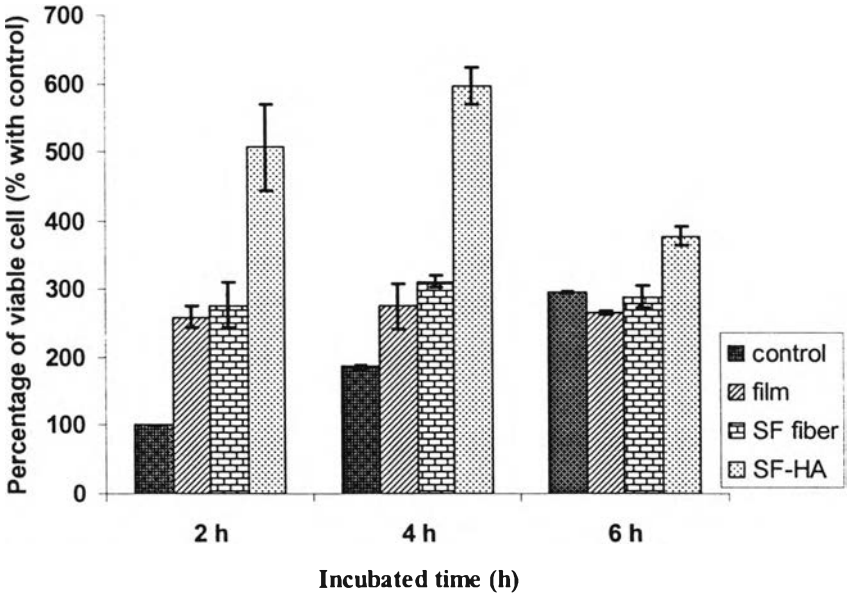

Figure 4.4 Attachment of HaCaT on control, SF film, as-spun SF fibers and HA-coated SF fibers scaffolds as a function of time in culture.

The quantities of percentage of viable cells were listed in Table 4.5 and the normalized results are shown in Figure 4.4, which shows HaCaT cell attachment on scaffolding materials. The attachment of HaCaT on each type of the as-prepared scaffolding materials was better than on control at 2 and 4 hours. At 6 hours in culture, the number of HaCaT cells attached on control was higher than on SF fibers and SF film, while the SF-HA fibers showed higher absorbance. The number of percentage of HaCaT cells attached on control increased with increasing time in culture. Clearly, SF scaffold and SF scaffold coated with HA supported cell growth of HaCaT viable cells at 2 and 4 hour, while at 6 hours the number of cells were not significantly different in other materials. However, it can be concluded that the number of viable cells attached on SF-HA fibers were higher than those attached on SF fibers and SF film, respectively, at all time in culture for attachment.

Besides the investigation of cell attachment, cell proliferation was also investigated. HaCaT cell proliferation on scaffolding materials including control at 1, 2 and 3 days. As shown in Table 4.6, the morphology of proliferation of HaCaT cells on control, SF film, SF fibers and SF-HA fibers were observed that cell shape was flatter than in cell attachment time. The shape of HaCaT cells on SF fiber and SF-HA fiber scaffolds were similar, while the shape of HaCaT cells were also alike. When time in culture increased, HaCaT cell shape were more spread with increasing time.

From the results, it can be explained that HA can support HaCaT cell attachment because HA is a major constituent of the ECM that cells produce ECM for supporting attachment and growth. Cell attachment appears through receptor on surface cell which is called integrins. The integrin of cells link to ECM, therefore HA have the ability in supporting cell attachment. Moreover, electrospun SF fibers provide a higher level of surface area-to-volume ratio and porosity for cells to attach.

Table 4.6 SEM micrographs (500X) of the HaCaT cell proliferate on the surface of SF film, as-spun SF and SF-HA scaffolds comparison with control. The scale bar shown is 50 μm.

	Control	SF Film	SF fiber	SF-HA
1 day	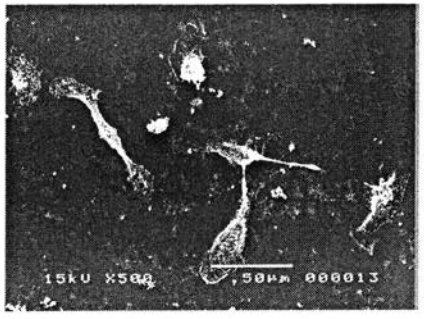	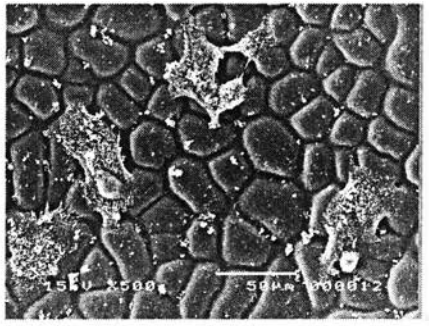	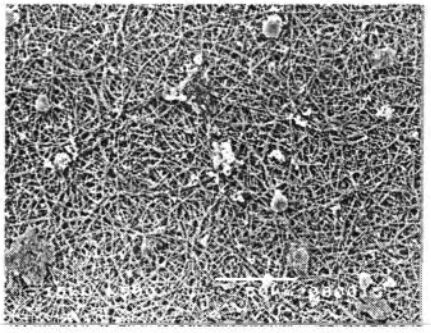	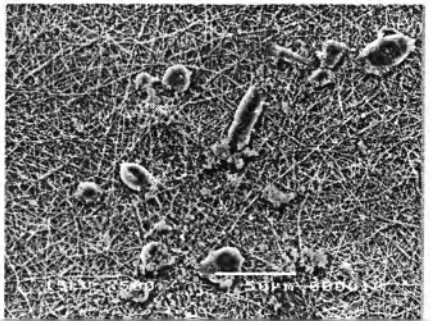
2 days	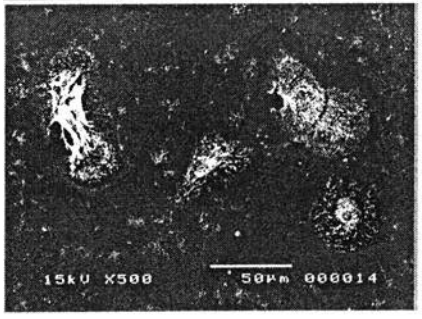	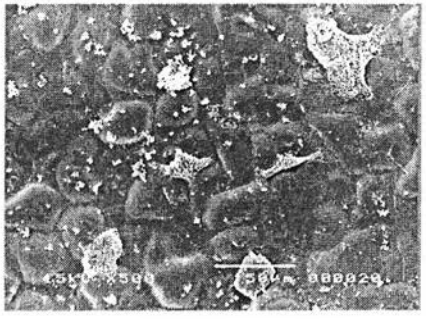	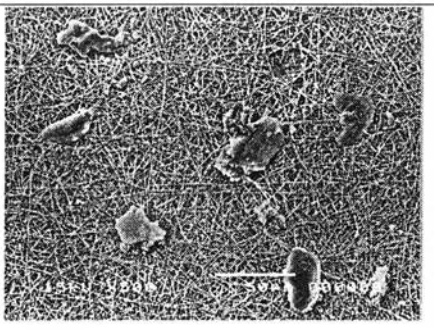	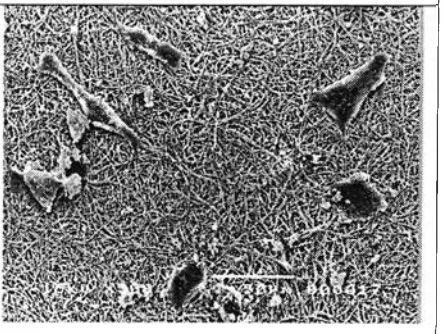

Table 4.6 (continued)

	Control	SF Film	SF fiber	SF-HA
3 days	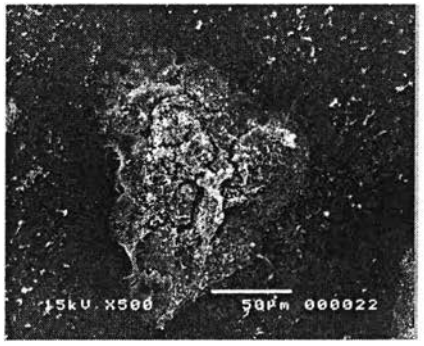	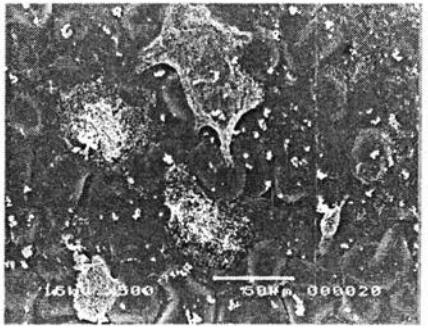	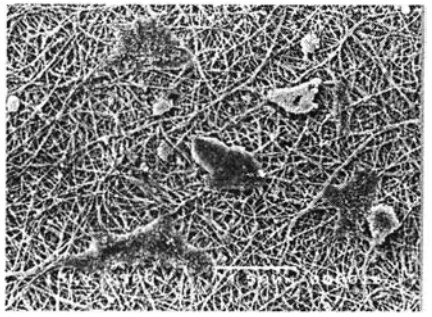	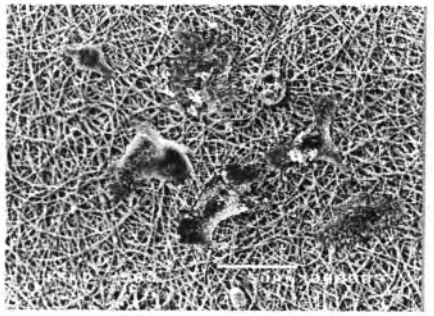

Table 4.7 Data shows the quantities (%) of percentage of viable HaCaT cell proliferated on each scaffolding material comparison with control.

Type	Absorbance			Percentage of viable cell (% with control)		
	1 day	2 days	3 days	1 day	2 days	3 days
Control	0.369	0.497	0.697	100 ± 4	135 ± 7	189 ± 9
SF film	0.391	0.409	0.381	106 ± 16	111 ± 17	103 ± 20
SF fiber	0.412	0.469	0.446	112 ± 11	127 ± 12	121 ± 8
SF-HA	0.512	0.557	0.457	139 ± 11	151 ± 12	124 ± 11

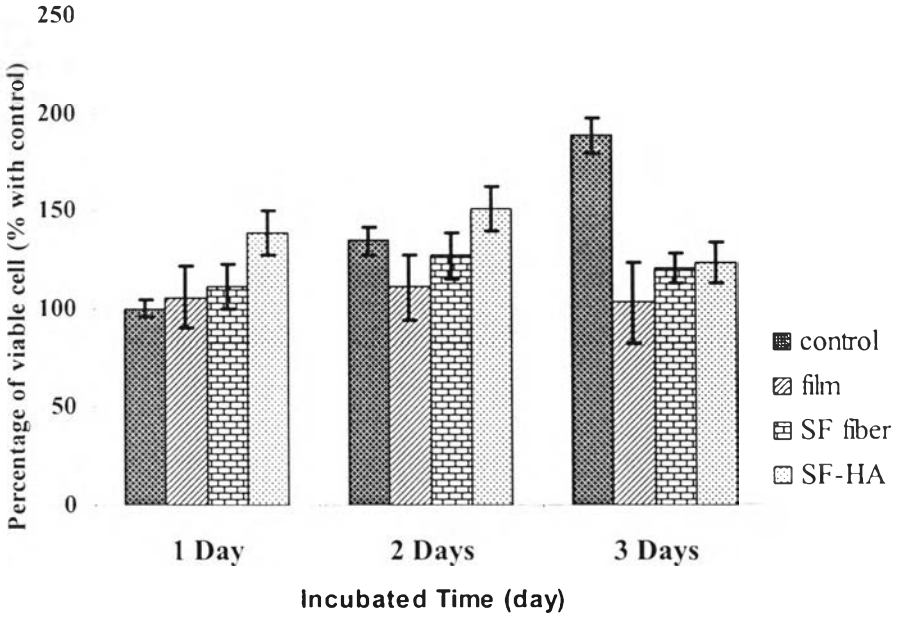

Figure 4.5 Proliferation of HaCaT cell on control, SF film, as-spun SF and HA-coated as-spun SF fibrous scaffolds as a function of time in culture.

The quantities of percentage of viable cells were listed in Table 4.7 and the normalized results are shown in Figure 4.5, which illustrates proliferation of HaCaT cell on materials including control. The trend of number of percentage of viable HaCaT cells on SF film, SF fibers and SF-HA fibers increased then decreased at 3 days while trend of

control increased with increasing time. SF-HA exhibited the greatest number of viable cells at 1 day. At 3 days in culture, the number of HaCaT cells can proliferate on control were higher than on SF fibers, SF-HA fibers, and SF film. Clearly, SF fibers and SF-HA fibers can support cell growth of HaCaT at 1 and 2 days while at 3 days the number of cells decreased comparing with the shorter times. It can be explained that the SF film, SF fibers, and SF-HA fibers supported cell proliferation better than control therefore the cell growth cycle on these materials was so fast that cell growth range falls into plateau phase. Cell growth is in the plateau phase when the growth rate of cell decreases or cell growth spreads completely.

4.5.2 HFF cells

Table 4.8 illustrates the attachment of HFF cells on each scaffold including control. Clearly, it was shown that the attachment of HFF cells on SF and SF-HA fibers at 2 h and 4 h was better than on the control and SF films. However, there was no significant difference among each sample at 6 h. From the SEM micrographs, cells on all scaffolding materials including control started showed the lamellipodia at 2 h and HFF shape was flat with increasing time in culture. This result supported the ability of HA in cell attachment.

Table 4.8 SEM micrographs of HFF attached on the surface of SF film, as-spun SF and SF-HA scaffolds comparison with control.

	Control	SF Film	SF fiber	SF-HA
2 h	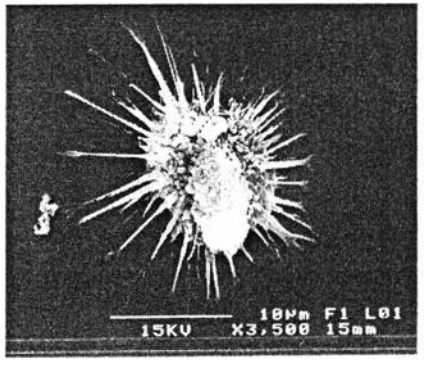 (3500X)	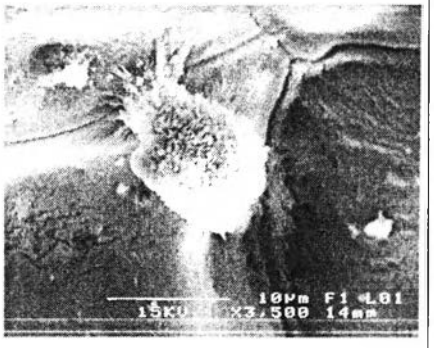 (3500X)	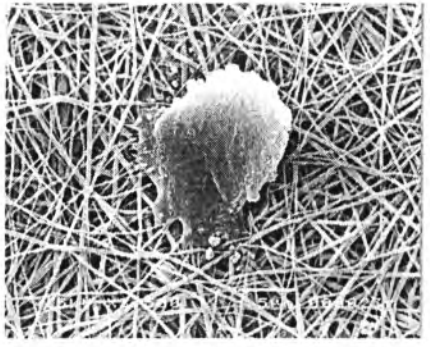 (3500X)	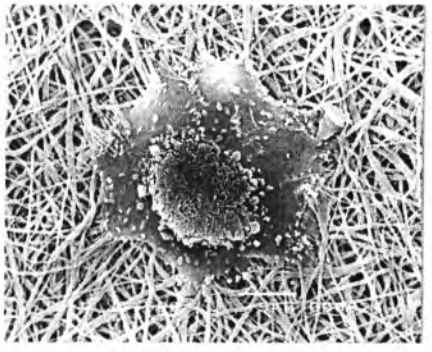 (3500X)
4 h	 (2000X)	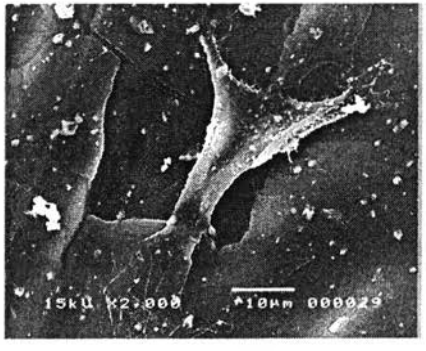 (2000X)	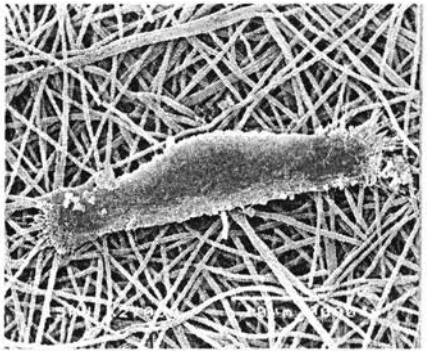 (2000X)	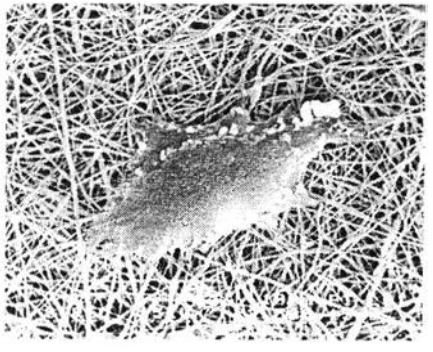 (2500X)

Table 4.8 (continued)

	Control	SF Film	SF fiber	SF-HA
6 h	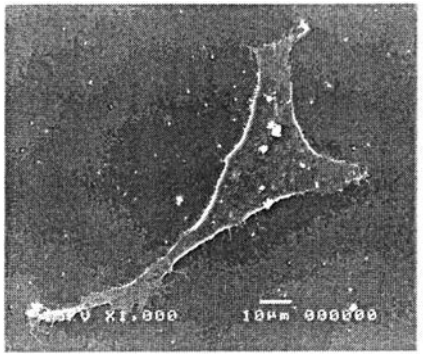 (1000X)	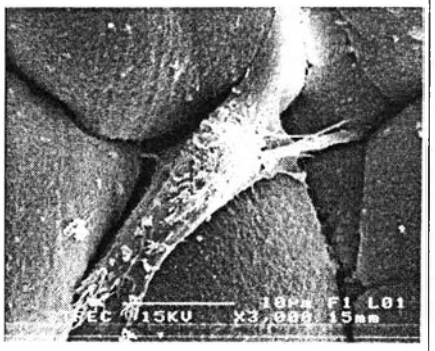 (3000X)	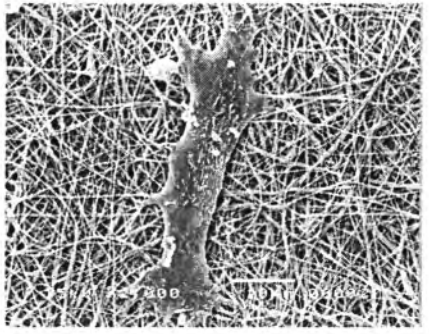 (2000X)	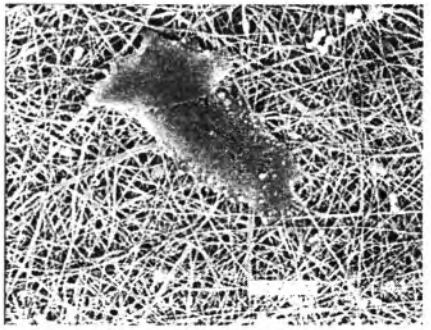 (1700X)

Table 4.9 Data shows the quantities (%) of percentage of viable HFF cell attached on each scaffolding material comparison with control.

Type	Absorbance			Percentage of viable cell (% with control)		
	2 h	4 h	6 h	2 h	4 h	6 h
Control	0.099	0.156	0.138	100 ± 26	158 ± 33	139 ± 18
SF film	0.211	0.210	0.158	213 ± 15	212 ± 4	160 ± 8
SF fiber	0.222	0.250	0.183	224 ± 14	253 ± 5	185 ± 2
SF-HA	0.349	0.339	0.329	352 ± 18	342 ± 24	332 ± 4

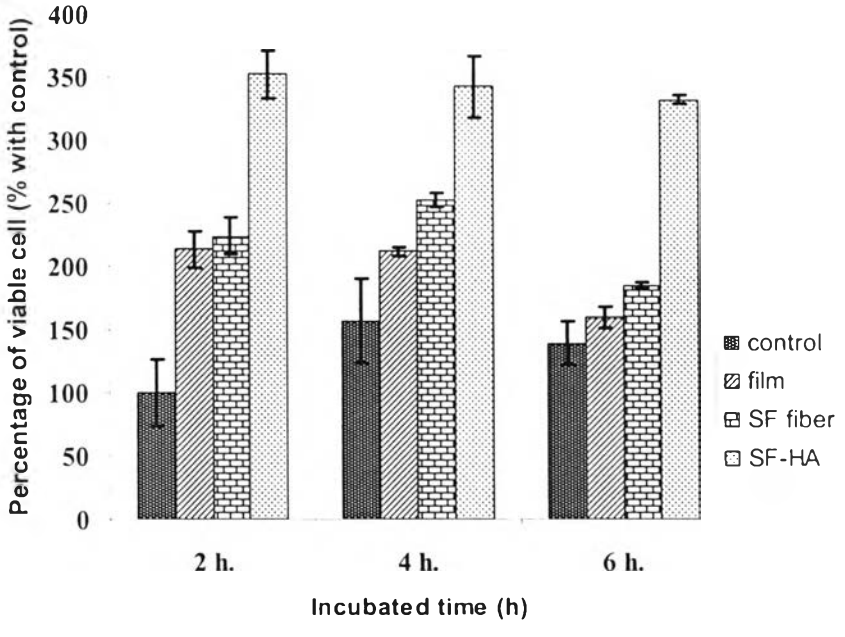

Figure 4.6 Attachment of HFF cell on control, SF film, as-spun SF and SF-HA scaffolds as a function of time in culture.

The quantities of percentage of viable cells were listed in Table 4.9 and the normalized results are shown in Figure 4.6, which shows the number HFF cells attached on scaffolding materials. As can be seen at 2, 4 and 6 hours in culture time, the number of viable cells on SF-HA was greater than on SF fibers and SF films, respectively. The

number of viable HFF cells on SF-HA was the highest among the scaffolding materials investigated including control at all time in culture. In addition, the number of viable cells increased at 2 and 4 hours and then decreased at 6 hours in culture. Further, trend of number of viable HFF cells on all type of scaffolding materials at 2 and 4 hours the number of viable cells increased then decreased at 6 hours in culture time. The reason can be explained in a similar manner to the attachment of HaCaT cells.

Table 4.10 SEM micrographs (500X) of HFF cells proliferated on the surface of SF film, as-spun SF and SF-HA scaffolds comparison with control.

	Control	SF Film	SF fiber	SF-HA
1 day	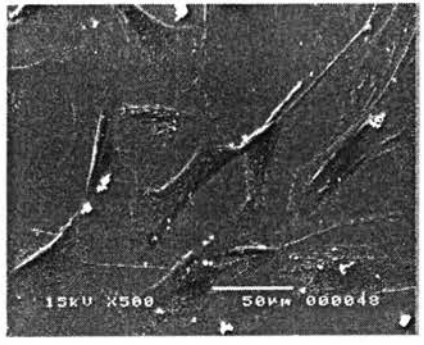	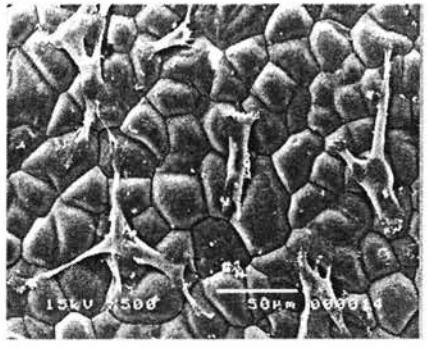	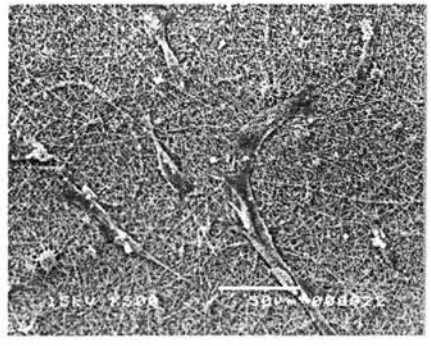	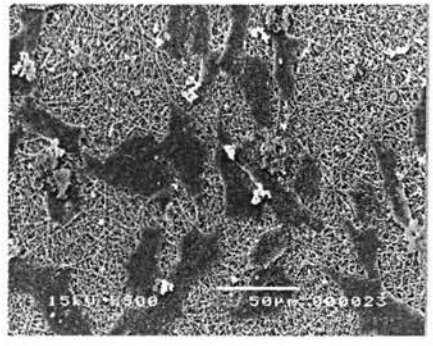
2 days	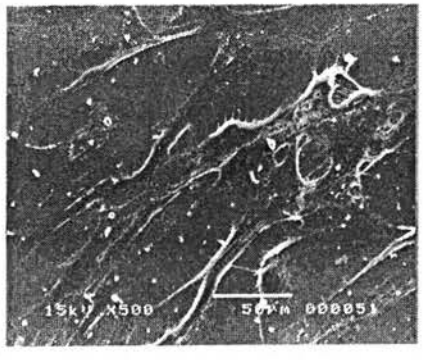	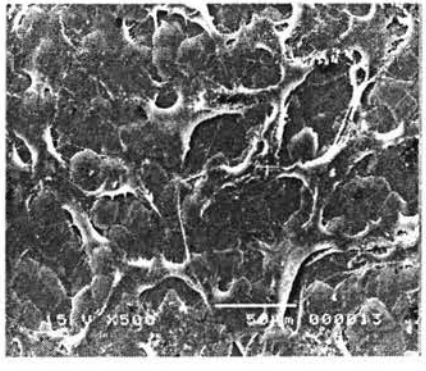	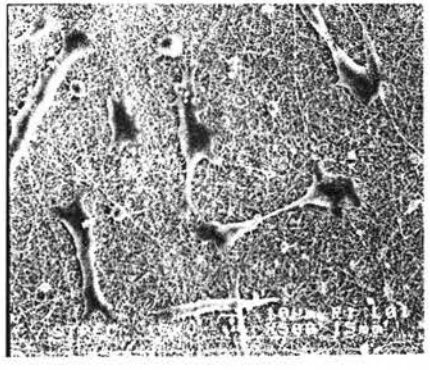	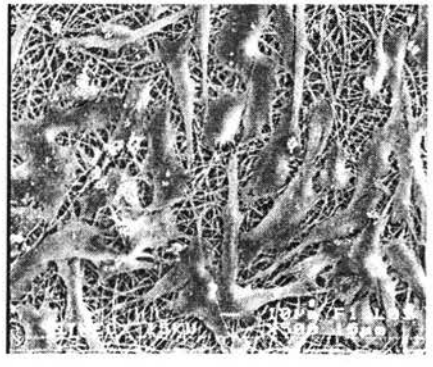

Table 4.10 (continued)

	Control	SF Film	SF fiber	SF-HA
3 days	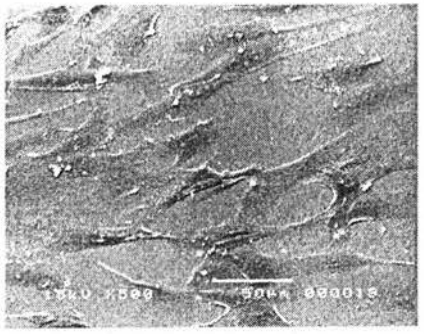		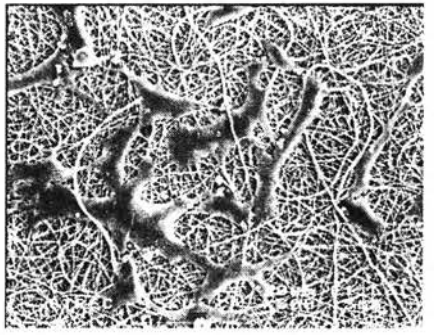	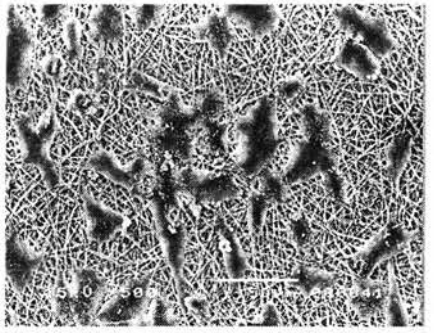

As indicated in Table 4.10, the area on which the cells occupied increased with increasing time in culture. In addition, each HFF cells contacted on the surface through the lamellipodia. Moreover, at longer time in culture cell phenotype expanded more than at shorter time. At 1 day, the cell phenotypes of electrospun SF-HA scaffolds tended to expand more than other type scaffolds. While at 2 and 3 days cell phenotypes were not quite different on all types of scaffolding materials.

Table 4.11 Data shows the quantities (%) of percentage of viable HFF cell proliferated on each scaffolding material comparison with control.

Type	Absorbance			Percentage of viable cell (% with control)		
	1 day	2 days	3 days	1 day	2 days	3 days
Control	0.398	0.497	0.721	100 ± 4	125 ± 7	181 ± 0.2
SF film	0.355	0.458	0.431	89 ± 4	115 ± 8	108 ± 17
SF fiber	0.412	0.469	0.465	104 ± 10	118 ± 5	117 ± 5
SF-HA	0.542	0.557	0.472	136 ± 8	140 ± 0.4	119 ± 0.3

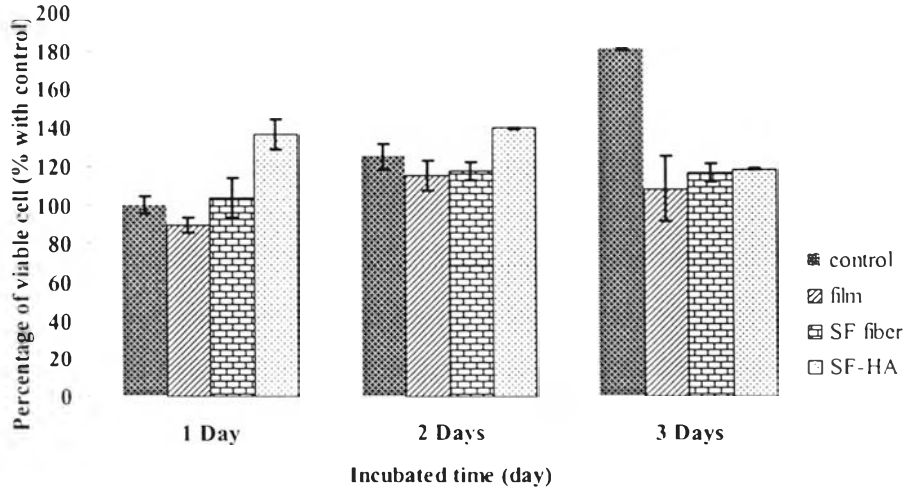

Figure 4.7 Proliferation of HFF cell on control, SF film, as-spun SF and SF-HA scaffolds as a function of time in culture.

The quantities of percentage of viable cells were listed in Table 4.11 and the normalized results are shown in Figure 4.7, which illustrates proliferation of HFF cell proliferation on scaffolding materials including control at 1, 2 and 3 days. From this figure, the number of viable cells of control tended to increase with increasing time in culture, while film, SF and SF-HA tended to increase at 1 and 2 days then slightly decreased at 3 days. It was also found that at 3 days the proliferation of HFF cells on controls was significantly better than on the film, SF and SF-HA. However, comparing with all the as-prepared scaffolding materials at all time in culture, it was found that the percentage of viable proliferated HFF cells on SF-HA were greater than SF fibers and SF films, respectively. The same reason with the proliferation of HaCaT cells could be used.